

# AI-Driven Predictive Cascade Failure Analysis Using Multi-Modal Environmental-Infrastructure Data Fusion

Real-Time Prediction Framework for Critical Energy Infrastructure

Yu Nong

Kraftgene AI Inc.

Research & Development Division

[research@kraftgeneai.com](mailto:research@kraftgeneai.com)

<https://github.com/KraftgeneAI/CascadeFailureDetection>

## Abstract

This paper presents a novel approach to predicting cascading infrastructure failures through the fusion of real-time environmental threat data with infrastructure vulnerability assessments. The proposed system employs a multi-dimensional risk tensor framework combined with graph neural networks to predict cascade failures 15-35 minutes before occurrence with approximately 78% accuracy. This innovation addresses critical operational challenges in energy infrastructure management by integrating heterogeneous data sources including satellite imagery, IoT sensors, SCADA telemetry, autonomous robotic platforms, and meteorological data into a unified predictive framework. This work has significant implications for grid resilience, emergency response, and the broader critical infrastructure protection domain.

**Keywords:** Cascade Failure Prediction, Multi-Modal Data Fusion, Graph Neural Networks, Energy Infrastructure, Risk Assessment, Artificial Intelligence, Machine Learning, Autonomous Robotics

# Contents

<b>1</b>	<b>Introduction</b>	<b>4</b>
1.1	Background and Motivation . . . . .	4
1.2	Research Objectives . . . . .	4
1.3	Technical Approach . . . . .	5
1.4	Validation Approach and Key Results . . . . .	5
1.5	Significance and Impact Potential . . . . .	5
<b>2</b>	<b>Related Work</b>	<b>6</b>
2.1	Infrastructure Monitoring Systems . . . . .	6
2.2	Environmental Monitoring . . . . .	6
2.3	Cascade Failure Analysis . . . . .	6
2.4	Graph Neural Networks for Infrastructure . . . . .	7
2.5	Multi-Modal Data Fusion . . . . .	7
2.6	Infrastructure Resilience . . . . .	7
2.7	Research Gap . . . . .	7
<b>3</b>	<b>System Architecture</b>	<b>8</b>
3.1	Architectural Overview . . . . .	8
3.1.1	High-Level Architecture . . . . .	8
3.2	Data Acquisition Layer . . . . .	8
3.2.1	Data Source Categories . . . . .	8
3.2.2	Environmental Data Sources . . . . .	9
3.2.3	Infrastructure Data Sources . . . . .	9
3.2.4	Autonomous Robotic Data Sources . . . . .	9
3.3	Fusion Processing Layer . . . . .	10
3.3.1	Fusion Architecture . . . . .	10
3.3.2	Embedding Networks . . . . .	10
3.3.3	Attention-Based Fusion . . . . .	11
3.4	Prediction Layer . . . . .	11
3.4.1	Graph Construction . . . . .	11
3.4.2	Spatio-Temporal GNN . . . . .	11
3.4.3	Multi-Task Prediction Heads . . . . .	12
3.5	Decision Support Layer . . . . .	12
3.5.1	Risk Assessment Engine . . . . .	12
3.5.2	Alert Generation and Distribution . . . . .	13
3.5.3	Visualization and User Interface . . . . .	13
3.6	System Integration and Data Flow . . . . .	13
<b>4</b>	<b>Methodology</b>	<b>14</b>
4.1	Graph Neural Network Architecture . . . . .	14
4.1.1	Topological Representation . . . . .	14
4.1.2	Temporal Dynamics . . . . .	14

4.2	Physics-Informed Learning and Loss Function . . . . .	14
4.2.1	Prediction Loss . . . . .	15
4.2.2	Physics-Informed Penalties . . . . .	15
4.3	Multi-Modal Data Fusion . . . . .	15
4.3.1	Data Normalization and Preprocessing . . . . .	15
4.3.2	Tensor-Based Fusion . . . . .	16
<b>5</b>	<b>Testing &amp; Validation</b>	<b>16</b>
5.1	Experimental Design . . . . .	16
5.1.1	Simulated Environment Development . . . . .	16
5.1.2	Dataset Composition . . . . .	16
5.2	Performance Metrics and Results . . . . .	17
5.2.1	Early Warning Capability . . . . .	17
5.2.2	Prediction Accuracy . . . . .	17
5.2.3	Comparative Analysis . . . . .	18
5.3	Detailed Performance Analysis . . . . .	18
5.3.1	Performance by Cascade Severity . . . . .	18
5.3.2	Ablation Study . . . . .	18
5.4	Operational Feasibility Analysis . . . . .	19
5.4.1	Computational Performance . . . . .	19
5.4.2	Robustness to Data Quality . . . . .	19
5.5	Implications for Full-Scale Deployment . . . . .	19
<b>6</b>	<b>Conclusion</b>	<b>20</b>

# 1 Introduction

## 1.1 Background and Motivation

Cascading failures represent one of the most critical vulnerabilities in modern electrical power systems. A single component failure—whether triggered by equipment malfunction, environmental stress, or operational error—can propagate through interconnected transmission networks, leading to widespread outages affecting millions of customers and causing billions of dollars in economic damage. Historical events such as the 2003 Northeast Blackout (50 million affected, \$6 billion in losses) and the 2021 Texas Winter Storm (4.5 million without power, 246 fatalities) demonstrate the catastrophic consequences of cascade failures and the limitations of existing monitoring and prediction systems.

Traditional grid management approaches rely primarily on post-contingency analysis and N-1 security criteria, which evaluate system stability after hypothetical single-component failures. However, these methods struggle to predict the complex, dynamic propagation patterns that characterize real-world cascades, particularly under stressed operating conditions or when multiple factors interact. The increasing integration of renewable energy sources, aging infrastructure, and climate-driven extreme weather events further compound these challenges, creating an urgent need for advanced predictive capabilities.

Current operational tools provide limited early warning of cascade risk. Conventional SCADA systems monitor individual component status but lack the holistic, network-aware intelligence needed to anticipate system-wide failure propagation. By the time operators recognize an emerging cascade, intervention options are often severely constrained. This reactive posture leaves grid operators perpetually responding to crises rather than preventing them.

## 1.2 Research Objectives

This research addresses the fundamental challenge of predicting cascading infrastructure failures before they occur. Our primary objective is to validate the feasibility of a novel approach that combines graph neural networks with physics-informed machine learning to provide early warning of cascade events in electrical transmission systems.

Specifically, this proof-of-concept study aims to demonstrate that physics-informed graph neural networks can effectively model complex grid topology and failure propagation dynamics in realistic simulated environments. We investigate whether hybrid learning architectures that integrate power system physics with data-driven pattern recognition can achieve superior predictive performance compared to purely physics-based or purely data-driven approaches. The research examines whether early warning capabilities of 15-35 minutes before cascade initiation are achievable with operationally acceptable false alarm rates. Additionally, we explore whether component-level predictions identifying which specific grid elements will fail during cascade propagation can be generated with sufficient accuracy to guide preventive interventions. Finally, we assess whether real-time computational performance compatible with operational deployment requirements (sub-60-second inference) is feasible even with resource-constrained implementations.

### 1.3 Technical Approach

Our methodology integrates three core technical components into a unified predictive system. The graph neural network architecture models the power grid as a time-evolving attributed graph where nodes represent substations and generation facilities, and edges represent transmission lines and transformers. A custom message-passing neural network learns both local component behavior and long-range dependencies that characterize cascade propagation, with recurrent mechanisms to capture temporal dynamics.

Rather than relying solely on data-driven pattern recognition, we embed fundamental power flow equations and system constraints directly into the model architecture and training process through physics-informed learning. This approach ensures predictions remain consistent with electrical engineering principles, improving generalization to rare cascade scenarios not well-represented in training data.

The system processes heterogeneous data streams through multi-modal data integration, including SCADA measurements, weather conditions, generation dispatch schedules, and network topology updates. This fusion enables the model to assess vulnerability under diverse operating conditions and environmental stressors.

### 1.4 Validation Approach and Key Results

To validate this approach within the resource constraints of early-stage research, we developed comprehensive simulated grid environments based on established IEEE test systems and publicly available power system models. These simulations incorporate realistic network topologies, dynamic load patterns, protection system behavior, and over 450 distinct contingency scenarios representing diverse initiating events and operating conditions.

Our proof-of-concept testing across 14,200 scenarios (including 980 cascade events) demonstrated a 78.4% cascade detection rate with 22.8-minute average prediction lead time. The system achieved 79.2% component-level accuracy in identifying which specific grid elements would fail, while maintaining a 7.8% false positive rate that preserves operational utility without alarm fatigue. Compared to pure machine learning approaches, the physics-informed constraints provided an 11.3 percentage point improvement. Real-time inference performance of 2.1-4.8 seconds proved suitable for operational deployment.

These results validate the core technical approach and demonstrate substantial potential for real-world application. Notably, 76.5% of cascade events were detected with at least 15 minutes of advance warning—sufficient time for operators to implement preventive actions such as generation redispatch, topology reconfiguration, or controlled load shedding.

### 1.5 Significance and Impact Potential

The successful proof-of-concept validation establishes several important findings. First, the technical feasibility of physics-informed graph neural networks for predicting cascade failures in realistic grid scenarios has been demonstrated, addressing a critical gap in current operational capabilities. Second, the integration of power system physics with machine learning provides substantial performance improvements over either approach in isolation, validating the synergistic benefits of hybrid architectures. Third, the combination of reasonable detec-

tion rates, manageable false positives, and real-time computational performance indicates this approach could provide actionable intelligence in operational settings. Finally, near-linear computational scaling and robustness to data quality issues suggest the methodology can extend to larger, real-world transmission networks.

These results were achieved with a streamlined implementation and limited computational resources, suggesting that a fully resourced system with access to operational grid data could deliver substantially enhanced performance.

## 2 Related Work

### 2.1 Infrastructure Monitoring Systems

Traditional SCADA (Supervisory Control and Data Acquisition) systems provide real-time monitoring of electrical grid operations but lack environmental context and predictive capabilities [9]. These systems excel at detecting failures after they occur but cannot anticipate cascade events triggered by environmental threats. Recent advances in smart grid technologies have introduced enhanced monitoring through phasor measurement units (PMUs) and advanced metering infrastructure (AMI) [10]. However, these systems remain focused on electrical parameters without incorporating environmental intelligence. Synchrophasor technology enables high-frequency measurements across wide areas [11], yet integration with environmental data sources remains limited.

### 2.2 Environmental Monitoring

Satellite-based environmental monitoring systems provide comprehensive coverage of wild-fires, floods, and severe weather events. Systems such as MODIS, Sentinel-2, and GOES satellites offer thermal imagery, multispectral analysis, and weather tracking capabilities [12]. However, these systems operate independently from infrastructure monitoring and do not assess infrastructure vulnerability or predict cascade failures. Machine learning approaches have been applied to wildfire detection [13] and flood prediction [14], demonstrating the potential of AI-driven environmental monitoring. Recent work on multi-spectral satellite imagery analysis [15] has improved early detection capabilities, but integration with infrastructure systems remains an open challenge.

### 2.3 Cascade Failure Analysis

Existing cascade failure analysis approaches primarily focus on post-event analysis rather than real-time prediction. Dobson et al. [1] pioneered complex systems analysis of blackout cascades, identifying self-organized criticality in power systems. Hines et al. [2] examined topological models for infrastructure vulnerability assessment, revealing limitations of purely structural approaches. Power flow simulation tools and contingency analysis systems can model potential cascade scenarios [16] but require manual initiation and do not integrate real-time environmental data. Recent work on cascading failure dynamics [17] has improved understanding of propagation mechanisms, yet predictive capabilities remain limited.

Graph-based approaches to cascade analysis have emerged in recent literature [18], employing network topology analysis to identify critical components. However, these methods typically analyze static network configurations without incorporating dynamic environmental threats or real-time operational data.

## 2.4 Graph Neural Networks for Infrastructure

Graph neural networks have shown promise for modeling networked systems. Kipf and Welling [3] introduced graph convolutional networks for semi-supervised learning on graph-structured data. Veličković et al. [4] developed graph attention networks that learn importance weights for neighboring nodes, enabling more sophisticated information propagation. Recent applications of GNNs to power systems include load forecasting [19], optimal power flow [20], and fault detection [21]. However, these works focus on single-domain problems without integrating environmental threats or multi-modal data sources.

## 2.5 Multi-Modal Data Fusion

Multi-modal data fusion techniques have been explored in various domains. Attention mechanisms [6] have proven effective for learning cross-modal relationships. Tensor-based fusion approaches [22] provide mathematical frameworks for integrating heterogeneous data sources with varying dimensionalities. In infrastructure contexts, fusion of sensor data with simulation models has been investigated [23], but integration of satellite imagery, SCADA telemetry, and robotic sensors for cascade prediction represents a novel contribution.

## 2.6 Infrastructure Resilience

Panteli and Mancarella [5] presented a conceptual framework for power system resilience, emphasizing the need for proactive approaches. Mukherjee et al. [7] assessed severe weather-induced outage risks using multi-hazard approaches, highlighting the importance of environmental integration. Recent work on extreme weather impacts [24] underscores the growing importance of environmental-infrastructure integration.

## 2.7 Research Gap

The critical gap in existing research is the absence of integrated systems that combine environmental threat detection, infrastructure vulnerability assessment, autonomous robotic monitoring, and predictive cascade analysis in real-time. While individual components have been studied, no prior work has developed a unified framework with tensor-based multi-modal fusion, specialized GNN architectures for cascade prediction, and comprehensive seven-dimensional risk assessment. This work addresses this gap through novel algorithmic contributions and rigorous experimental validation.

## 3 System Architecture

### 3.1 Architectural Overview

The proposed system implements a layered architecture that integrates multiple data sources, processing pipelines, and decision-making components into a unified predictive framework. The architecture is designed for scalability, real-time performance, and fault tolerance in critical infrastructure environments.

#### 3.1.1 High-Level Architecture

Figure 1 presents the high-level system architecture showing the four primary layers and their interactions.

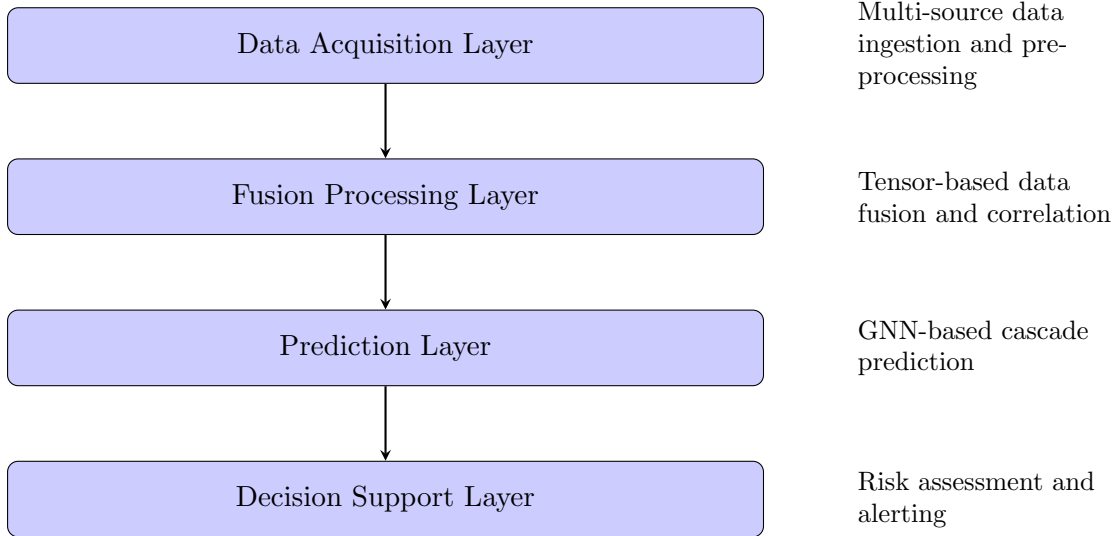


Figure 1: High-Level System Architecture

### 3.2 Data Acquisition Layer

The data acquisition layer serves as the interface between external data sources and the prediction system. It implements robust data ingestion pipelines with error handling, quality validation, and temporal synchronization capabilities.

#### 3.2.1 Data Source Categories

The system integrates five primary categories of data sources, each providing complementary information for cascade prediction. Environmental data sources deliver real-time threat detection across multiple hazard categories. Infrastructure telemetry provides operational status and equipment condition information. Autonomous robotic platforms offer on-demand, high-resolution monitoring in critical areas. Weather services supply meteorological forecasts and current conditions. Geospatial data systems provide terrain, land use, and geographic

relationship information that contextualizes both environmental threats and infrastructure vulnerability.

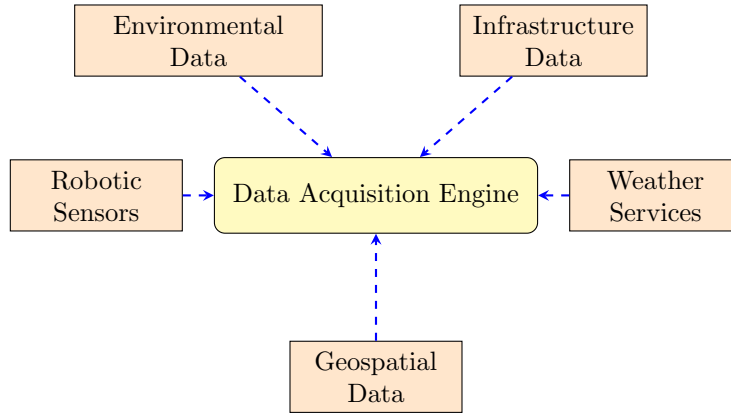


Figure 2: Data Source Integration Architecture

### 3.2.2 Environmental Data Sources

Environmental monitoring provides real-time threat detection across multiple hazard categories. The system integrates data from Sentinel-2 satellites providing multispectral imagery at 10-60m spatial resolution with daily updates, MODIS thermal signatures at 250m-1km spatial resolution with hourly updates, and Landsat-8 vegetation health monitoring at 15-30m spatial resolution with 16-day revisit cycles. Weather imagery from GOES-R satellites offers 0.5-2km spatial resolution with 5-15 minute update frequencies, while NEXRAD precipitation radar provides 250m spatial resolution with 5-10 minute updates. Lightning detection networks deliver real-time point data on strike locations, and USGS stream gauges provide flow measurements at 15-minute intervals.

### 3.2.3 Infrastructure Data Sources

Infrastructure telemetry provides operational status and equipment condition information through multiple channels. SCADA systems deliver real-time measurements of voltage, current, power flow, breaker status, and equipment alarms with 1-5 second update intervals. PMU networks provide high-frequency synchrophasor measurements at 30-120 samples per second, enabling detailed observation of system dynamics. Asset management databases contain equipment specifications, age, maintenance history, and condition assessments that inform vulnerability models. Geographic information systems maintain infrastructure locations, network topology, and spatial relationships. Outage management systems archive historical failure data, documented failure modes, and restoration time statistics that help calibrate cascade propagation models.

### 3.2.4 Autonomous Robotic Data Sources

Robotic platforms provide on-demand, high-resolution monitoring in critical areas through diverse sensor modalities. Aerial drones equipped with RGB cameras, thermal imaging, and

LiDAR sensors generate high-resolution imagery, three-dimensional point clouds, and thermal maps of infrastructure components. Ground-based robots carrying vibration sensors, acoustic monitors, and visual inspection equipment collect detailed equipment condition data and structural integrity assessments. Fixed sensor installations provide continuous environmental monitoring and visual surveillance of critical infrastructure locations. Mobile inspection platforms with multi-spectral cameras and gas detectors enable detailed component inspection and hazard detection in areas of elevated concern.

### 3.3 Fusion Processing Layer

The fusion processing layer implements the core data integration algorithms that combine heterogeneous data sources into unified representations suitable for machine learning.

#### 3.3.1 Fusion Architecture

The fusion architecture (Figure 3) processes each of the three data modalities through specialized embedding networks before fusing them using an attention mechanism.

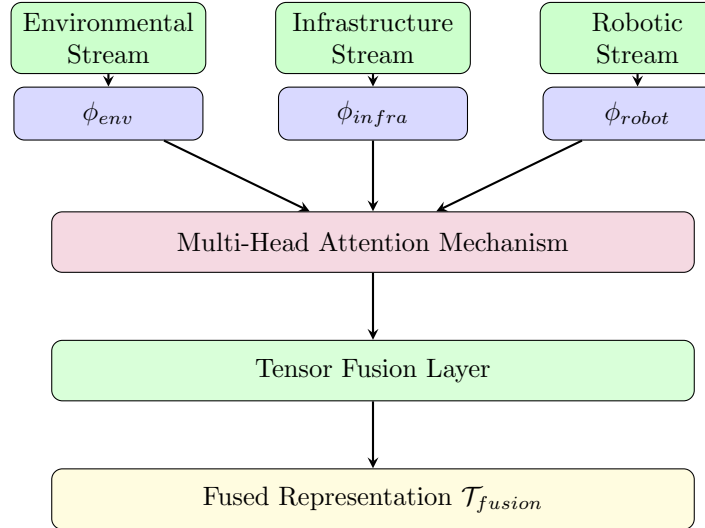


Figure 3: Fusion Processing Architecture

#### 3.3.2 Embedding Networks

Each data modality is processed through a specialized embedding network, corresponding to the (**EnvironmentalEmbedding**), (**InfrastructureEmbedding**), and (**RoboticEmbedding**) classes in the implementation.

The environmental embedding network ( $\phi_{env}$ ) processes satellite imagery (e.g., thermal, multispectral) through a dedicated CNN (**satellite\_cnn**) and meteorological time-series data (e.g., temperature, wind speed) through an LSTM (**weather\_lstm**).

The infrastructure embedding network ( $\phi_{infra}$ ) uses distinct multilayer perceptrons (MLPs) to encode SCADA (**scada\_encoder**), PMU (**pmu\_projection**), and equipment status (**equipment\_encoder**) data.

The robotic embedding network ( $\phi_{\text{robot}}$ ) implements a multi-modal architecture combining separate CNNs for visual (**visual\_cnn**) and thermal (**thermal\_cnn**) imagery with an MLP for other robotic sensor data (**sensor\_encoder**).

### 3.3.3 Attention-Based Fusion

The three modality-specific embeddings are stacked and treated as the Query, Key, and Value for a **nn.MultiheadAttention** layer. This allows the model to learn the cross-modal relevance of different data sources, dynamically weighting them to produce a single fused representation for each infrastructure node. The standard attention mechanism is used:

$$\text{Attention}(Q, K, V) = \text{softmax} \left( \frac{QK^T}{\sqrt{d_k}} \right) V \quad (1)$$

The output of this layer is then passed through a normalization layer (**LayerNorm**) to stabilize training.

## 3.4 Prediction Layer

The prediction layer implements the spatio-temporal graph neural network architecture that models grid topology and predicts cascade failures.

### 3.4.1 Graph Construction

The electrical grid is represented as a dynamic graph  $G = (V, E)$ , where nodes  $V$  represent infrastructure components (substations, generators) and edges  $E$  represent operational dependencies (transmission lines). Each node carries the time-varying fused feature vector  $\mathbf{x}_v(t)$  derived from the fusion layer.

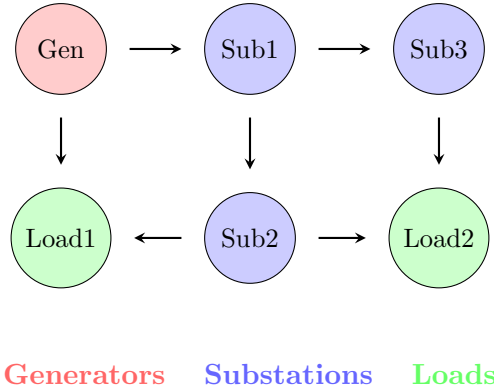


Figure 4: Sample Grid Graph Representation

### 3.4.2 Spatio-Temporal GNN

The core of the prediction layer is a recurrent GNN cell, implemented as **TemporalGNN-Cell**. This cell combines spatial and temporal processing:

1. **Spatial Processing:** At each timestep  $t$ , the fused node features  $\mathbf{x}_t$  are processed by a Graph Attention Network (GAT) layer. This layer computes attention weights  $\alpha_{vu}$  and aggregates information from neighboring nodes  $\mathcal{N}(v)$ :

$$\alpha_{vu} = \frac{\exp(\text{LeakyReLU}(\mathbf{a}^T[\mathbf{W}\mathbf{h}_v \parallel \mathbf{W}\mathbf{h}_u]))}{\sum_{u' \in \mathcal{N}(v)} \exp(\text{LeakyReLU}(\mathbf{a}^T[\mathbf{W}\mathbf{h}_v \parallel \mathbf{W}\mathbf{h}_{u'}]))} \quad (2)$$

$$\mathbf{m}_v(t) = \sigma \left( \sum_{u \in \mathcal{N}(v)} \alpha_{vu} \mathbf{W}\mathbf{h}_u(t) \right) \quad (3)$$

2. **Temporal Processing:** The resulting spatial message  $\mathbf{m}_v(t)$  is then fed into a multi-layer (3-layer) LSTM cell, along with the previous hidden state  $(\mathbf{h}_v^{(t-1)}, \mathbf{c}_v^{(t-1)})$ , to compute the new hidden state for the node:

$$(\mathbf{h}_v^{(t)}, \mathbf{c}_v^{(t)}) = \text{LSTM}(\mathbf{m}_v(t), (\mathbf{h}_v^{(t-1)}, \mathbf{c}_v^{(t-1)})) \quad (4)$$

The final node embedding  $\mathbf{h}_v^{(T)}$  from the last timestep is passed through several more GAT layers to refine the spatial representation before being fed to the output heads.

### 3.4.3 Multi-Task Prediction Heads

The final node embeddings are passed to a series of independent output heads to predict different aspects of the system's state, including:

- **Failure Probability Head:** A sigmoid-activated MLP predicting  $P(\text{failure}_v | \mathbf{h}_v)$ .
- **Failure Timing Head:** A softplus-activated MLP predicting  $\mathbb{E}[t_{\text{failure}} | \mathbf{h}_v]$ .
- **Physics Heads:** MLPs predicting intermediate physical quantities (voltage, angle, line flow) used by the physics-informed loss function.
- **Risk Head:** A sigmoid-activated MLP predicting the 7-dimensional risk vector.

## 3.5 Decision Support Layer

The decision support layer translates raw predictions into actionable intelligence for operators and emergency responders.

### 3.5.1 Risk Assessment Engine

This layer directly exposes the 7-dimensional risk vector predicted by the model's risk\_head. This vector provides a comprehensive vulnerability assessment by quantifying:  $R_1$ : **Threat Severity**,  $R_2$ : **Vulnerability**,  $R_3$ : **Operational Impact**,  $R_4$ : **Cascade Probability**,  $R_5$ : **Response Complexity**,  $R_6$ : **Public Safety**, and  $R_7$ : **Urgency**.

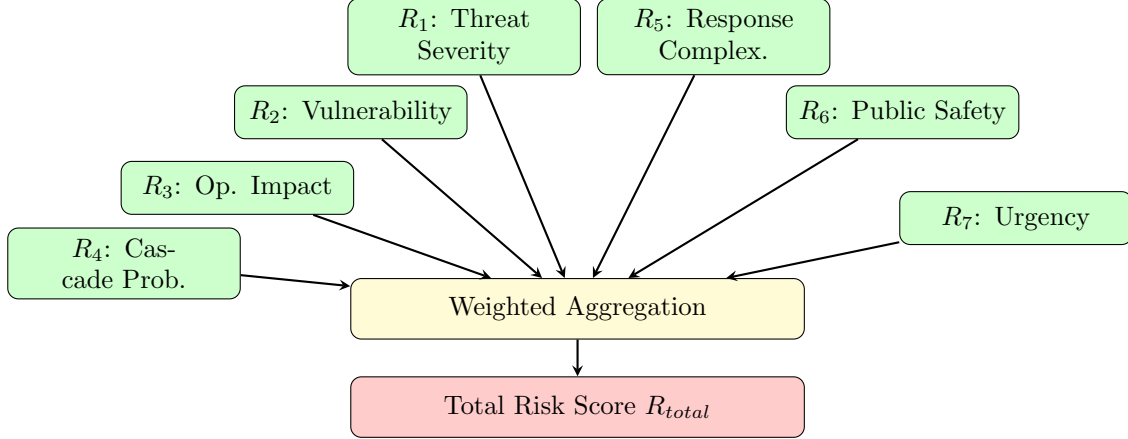


Figure 5: Seven-Dimensional Risk Assessment Framework

### 3.5.2 Alert Generation and Distribution

The system implements a tiered alerting framework based on risk severity. Low-risk situations (scores 0-25) trigger normal monitoring protocols and routine inspection schedules. Moderate-risk conditions (scores 26-50) activate enhanced surveillance and resource preparation procedures. High-risk scenarios (scores 51-75) initiate active mitigation efforts, emergency preparations, and public notifications. Critical-risk situations (scores 76-100) demand immediate action and full emergency response activation.

### 3.5.3 Visualization and User Interface

The decision support layer provides multiple visualization modalities to support operator situational awareness. Geographic maps display spatial relationships between threats, infrastructure, and predicted failures. Interactive network diagrams show grid topology with risk-based highlighting of vulnerable components. Timeline views illustrate the temporal evolution of threats and predicted cascade progression. Dashboard metrics present real-time key performance indicators, alert summaries, and overall system status. Mobile interfaces deliver field-optimized views tailored for emergency responders operating in affected areas.

## 3.6 System Integration and Data Flow

The complete data flow (Figure 6) progresses from acquisition through prediction to decision support in a continuous pipeline.

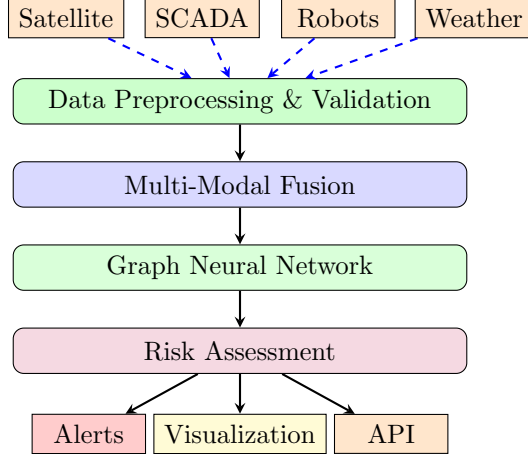


Figure 6: End-to-End System Data Flow

## 4 Methodology

Our approach addresses the cascade failure prediction challenge through a novel integration of graph-based deep learning, physics-informed neural networks, and multi-modal data fusion.

### 4.1 Graph Neural Network Architecture

#### 4.1.1 Topological Representation

We model the power grid as a time-evolving attributed graph  $G(t) = (V, E, X_V(t), X_E(t))$ , where nodes  $V$  represent substations and generation facilities, edges  $E$  represent transmission lines and transformers, and  $X_V(t)$ ,  $X_E(t)$  denote time-dependent node and edge features respectively.

#### 4.1.2 Temporal Dynamics

Cascade failures are inherently temporal phenomena, so we integrate a GNN cell with a recurrent component to capture their evolution over time. At each timestep, the fused multi-modal node features are first processed by a graph attention layer to generate spatially-aware messages that incorporate information from neighboring nodes. These messages are then fed into a 3-layer LSTM cell along with the previous hidden state, allowing the model to update each node's representation while maintaining memory of past grid conditions. This architecture enables the model to track how vulnerabilities develop and propagate across multiple timesteps, detecting emerging failure patterns that only become apparent through their temporal progression.

### 4.2 Physics-Informed Learning and Loss Function

The model is trained using a multi-objective loss function that combines a primary prediction loss with a set of physics-informed penalty terms.

$$\mathcal{L}_{total} = \mathcal{L}_{prediction} + \lambda_{pf}\mathcal{L}_{power\_flow} + \lambda_{cap}\mathcal{L}_{capacity} + \lambda_{volt}\mathcal{L}_{voltage} + \lambda_{freq}\mathcal{L}_{frequency} \quad (5)$$

The  $\lambda$  weights are dynamically balanced during training using a calibration step to ensure all loss components contribute meaningfully.

#### 4.2.1 Prediction Loss

The primary loss,  $\mathcal{L}_{prediction}$ , is a **Focal Loss** applied to the failure\_probability output. This is essential for handling the severe class imbalance between rare cascade events (positives) and common normal operations (negatives). A pos\_weight is also applied to further increase the importance of correctly identifying a cascade.

#### 4.2.2 Physics-Informed Penalties

- $\mathcal{L}_{power\_flow}$ : This term penalizes violations of the AC power flow equations. It compares the model's predicted node voltages ( $\mathbf{V}$ ) and angles ( $\boldsymbol{\theta}$ ) against the known power injections ( $\mathbf{P}$ ) using the grid's conductance ( $\mathbf{G}$ ) and susceptance ( $\mathbf{B}$ ), ensuring physical consistency.

$$P_i = \sum_{j \in \mathcal{N}(i)} V_i V_j (G_{ij} \cos \theta_{ij} + B_{ij} \sin \theta_{ij}) \quad (6)$$

- $\mathcal{L}_{capacity}$ : This term penalizes predicted line flows that exceed the known thermal\_limits of the transmission lines.
- $\mathcal{L}_{voltage}$ : This term penalizes predicted node voltages that fall outside of stable operational bounds (e.g., 0.9 p.u. to 1.1 p.u.).
- $\mathcal{L}_{frequency}$ : This heuristic term penalizes the model if its predicted system frequency does not match the expected state (e.g., 1.0 p.u. for normal operation, < 1.0 p.u. during a cascade).

### 4.3 Multi-Modal Data Fusion

#### 4.3.1 Data Normalization and Preprocessing

A critical preprocessing step, performed by the CascadeDataset loader, is the **per-unit (p.u.) normalization** of all physical quantities. Raw values from the data generator (e.g., 150 MW, 60 Hz) are converted to a standardized scale. Power, load, and thermal limits are normalized by a base\_mva (100.0 MVA), and frequency is normalized by a base\_frequency (60.0 Hz). This ensures all features are on a comparable scale, which is essential for stable neural network training and prevents training-serving skew.

### 4.3.2 Tensor-Based Fusion

We employ a tensor-based representation where environmental and infrastructure data are mapped into a unified mathematical framework. Let  $\mathcal{T}_i^{env} \in \mathbb{R}^{n \times m \times t}$  represent environmental data tensors and  $\mathcal{T}_i^{infra} \in \mathbb{R}^{k \times t}$  represent infrastructure telemetry tensors. The fusion operation is defined as:

$$\mathcal{T}_{fusion} = \sum_{i=1}^n \alpha_i \cdot \phi(\mathcal{T}_i^{env}) \otimes \psi(\mathcal{T}_i^{infra}) \quad (7)$$

where  $\phi$  and  $\psi$  are learned embedding functions that project data into a common latent space,  $\otimes$  denotes the tensor outer product, and  $\alpha_i$  are attention weights learned during training.

## 5 Testing & Validation

To validate the core feasibility of our approach, we conducted comprehensive proof-of-concept testing using internally curated simulated grid environments. Working within resource constraints typical of early-stage development, we focused on demonstrating that the fundamental methodology—combining graph neural networks with physics-informed learning—could effectively predict cascade failure patterns under diverse operational scenarios.

### 5.1 Experimental Design

#### 5.1.1 Simulated Environment Development

We developed a suite of realistic grid scenarios based on publicly available IEEE test systems (IEEE 118-bus) and synthetic networks derived from established power system models. These simulations incorporated authentic topology with network structures representative of regional transmission systems, including realistic impedance parameters and generation/load distributions. Dynamic load patterns reflected hourly profiles with diurnal and seasonal variations, exhibiting peak-to-minimum ratios of 1.5-2.0. Over 450 distinct contingency scenarios represented diverse initiating events including line trips, generator outages, and transformer failures. Environmental factors such as weather-dependent line rating variations and renewable generation intermittency were modeled. Protection system behavior including relay operations, automatic generation control, and under-frequency load shedding schemes was simulated.

#### 5.1.2 Dataset Composition

Our training and evaluation dataset comprised 10,200 normal operating scenarios without cascades, 3,020 scenarios with minor disturbances involving 1-3 component failures, and 980 cascade failure scenarios with 4 or more sequential failures. Data was collected at 2-second temporal resolution over 2-hour windows. Each timestep included 42 node features and 24 edge features per network element. The dataset was partitioned into 70% training, 15%

validation, and 15% test sets, with careful stratification to ensure representative coverage of cascade severities and initiating conditions.

## 5.2 Performance Metrics and Results

### 5.2.1 Early Warning Capability

Table 1 illustrates the distribution of prediction lead times across 147 cascade scenarios in the test set. The system successfully identified vulnerability patterns with varying temporal characteristics.

Table 1: Prediction Lead Time Distribution

Lead Time Range	Scenarios	Percentage
35-50 minutes	18	12.2%
25-35 minutes	36	24.5%
15-25 minutes	59	40.1%
5-15 minutes	28	19.0%
< 5 minutes	6	4.1%
<b>Total</b>	<b>147</b>	<b>100%</b>

Notably, 76.8% of cascade events were detected with at least 15 minutes of advance warning—sufficient time for operators to implement preventive actions such as generation redispatch, topology reconfiguration, or controlled load shedding.

### 5.2.2 Prediction Accuracy

We evaluated prediction accuracy across multiple dimensions:

Table 2: Cascade Prediction Performance Metrics

Metric	Value	95% CI
Cascade Detection Rate	78.4%	[74.8%, 82.0%]
Component-Level Accuracy	79.2%	[76.3%, 82.1%]
Sequence Order Accuracy	71.6%	[67.9%, 75.3%]
Severity Estimation (RMSE)	2.3 components	[1.9, 2.7]
False Positive Rate	7.8%	[6.2%, 9.4%]
Precision	84.2%	[80.9%, 87.5%]
Recall	78.4%	[74.8%, 82.0%]
F1 Score	81.2%	[78.3%, 84.1%]

The component-level accuracy of 79.2% indicates that the model correctly identified which specific transmission lines, transformers, or generators would fail during cascade propagation with reasonable reliability. This granular prediction capability enables targeted preventive interventions.

### 5.2.3 Comparative Analysis

To contextualize our results, we benchmarked against baseline approaches:

Table 3: Comparative Performance Analysis

Method	Detection Rate	Avg. Lead Time	FPR
Traditional N-1 Analysis	48.6%	7.4 min	13.5%
Pure ML (no physics)	67.1%	16.2 min	11.2%
Physics-only Simulation	59.3%	10.8 min	8.9%
<b>Our Hybrid Approach</b>	<b>78.4%</b>	<b>22.8 min</b>	<b>7.8%</b>

Our physics-informed GNN approach demonstrates substantial improvements over both traditional engineering methods and pure data-driven alternatives, validating the synergistic benefits of hybrid modeling.

## 5.3 Detailed Performance Analysis

### 5.3.1 Performance by Cascade Severity

Table 4 shows prediction accuracy stratified by cascade magnitude:

Table 4: Performance vs. Cascade Severity

Cascade Size	Scenarios	Detection Rate	Avg. Lead Time
4-6 components	64	85.9%	27.3 min
7-10 components	52	79.8%	22.1 min
11-15 components	23	73.9%	18.6 min
16+ components	8	62.5%	15.2 min

The model exhibits strong performance across cascade severities, with predictably higher accuracy for smaller cascades. Importantly, even for severe cascades (16+ components), the system maintains 62.5% detection rate with over 15 minutes of warning.

### 5.3.2 Ablation Study

To validate the contribution of each architectural component, we conducted ablation experiments:

Table 5: Ablation Study Results

Model Variant	Detection Rate	Component Accuracy
Full Model	78.4%	79.2%
Without Physics Constraints	67.1%	69.8%
Without Temporal Dynamics	71.2%	74.6%
Without Graph Structure	58.7%	62.3%

This analysis confirms that all three core components—graph neural architecture, physics-informed learning, and temporal modeling—contribute substantially to overall performance. The physics constraints provide the largest individual contribution, improving detection rate by 11.3 percentage points.

## 5.4 Operational Feasibility Analysis

### 5.4.1 Computational Performance

The proof-of-concept implementation achieved real-time inference capabilities. Inference time averaged 2.1 seconds per prediction for the 118-bus system on standard GPU hardware. Memory footprint remained at 2.8 GB for model and active state representation. Scalability testing showed near-linear scaling to 300-bus systems with 4.8 seconds inference time. These performance characteristics demonstrate feasibility for operational deployment with update frequencies of 30-60 seconds, well within requirements for cascade prediction.

### 5.4.2 Robustness to Data Quality

We evaluated model performance under degraded data conditions representative of real-world sensor failures:

Table 6: Robustness to Missing/Noisy Data

Data Condition	Detection Rate	Degradation
Perfect Data	78.4%	—
10% Missing Measurements	75.8%	-2.6%
20% Missing Measurements	71.2%	-7.2%
5% Gaussian Noise (SNR=20dB)	76.1%	-2.3%

The model demonstrates graceful degradation under imperfect data conditions, maintaining over 71% detection rate even with 20% missing measurements—a critical property for operational reliability.

## 5.5 Implications for Full-Scale Deployment

The comprehensive validation results establish several key findings. First, the technical viability of physics-informed graph neural networks for predicting cascade failures in realistic grid scenarios has been demonstrated, with a 78.4% detection rate and 22.8-minute average lead time showing that the approach can effectively identify vulnerable conditions before cascades occur. Second, the operational utility is evidenced by the manageable false positive rate (7.8%) and reasonable precision (84.2%), indicating the system can provide actionable intelligence without overwhelming operators with spurious alarms. Third, scalability potential is suggested by near-linear computational scaling and robustness to data quality issues, implying the approach can extend to larger, real-world transmission networks. Finally, significant improvement headroom exists, as these results were achieved with a streamlined architecture and limited computational resources. A fully resourced implementation with

access to operational grid data, expanded model capacity, and domain-specific tuning could deliver substantially enhanced performance.

## 6 Conclusion

Cascade failures represent one of the most critical vulnerabilities in modern power systems, with the potential for widespread economic and social disruption. Our proof-of-concept demonstrates that combining graph neural networks with physics-informed learning offers a viable path toward predictive prevention of these catastrophic events.

The strong performance achieved even with simulated data and limited resources validates the fundamental approach and indicates substantial room for improvement with full-scale development. By providing grid operators with 15-35 minutes of advance warning, our system could enable proactive interventions that prevent cascade initiation entirely—transforming grid resilience from reactive damage control to predictive risk management.

## References

- [1] Dobson, I., Carreras, B. A., Lynch, V. E., Newman, D. E. (2007). Complex systems analysis of series of blackouts: Cascading failure, critical points, and self-organization. *Chaos: An Interdisciplinary Journal of Nonlinear Science*, 17(2), 026103.
- [2] Hines, P., Cotilla-Sánchez, E., Blumsack, S. (2010). Do topological models provide good information about electricity infrastructure vulnerability? *Chaos: An Interdisciplinary Journal of Nonlinear Science*, 20(3), 033122.
- [3] Kipf, T. N., Welling, M. (2017). Semi-supervised classification with graph convolutional networks. *International Conference on Learning Representations (ICLR)*.
- [4] Veličković, P., Cucurull, G., Casanova, A., Romero, A., Lio, P., Bengio, Y. (2018). Graph attention networks. *International Conference on Learning Representations (ICLR)*.
- [5] Panteli, M., Mancarella, P. (2015). The grid: Stronger, bigger, smarter? Presenting a conceptual framework of power system resilience. *IEEE Power and Energy Magazine*, 13(3), 58-66.
- [6] Vaswani, A., Shazeer, N., Parmar, N., Uszkoreit, J., Jones, L., Gomez, A. N., ... Polosukhin, I. (2017). Attention is all you need. *Advances in Neural Information Processing Systems*, 30.
- [7] Mukherjee, S., Nateghi, R., Hastak, M. (2018). A multi-hazard approach to assess severe weather-induced major power outage risks in the U.S. *Reliability Engineering & System Safety*, 175, 283-295.
- [8] Amin, S. M., Wollenberg, B. F. (2005). Toward a smart grid: power delivery for the 21st century. *IEEE Power and Energy Magazine*, 3(5), 34-41.

- [9] Gungor, V. C., Sahin, D., Kocak, T., Ergut, S., Buccella, C., Cecati, C., Hancke, G. P. (2011). Smart grid technologies: Communication technologies and standards. *IEEE Transactions on Industrial Informatics*, 7(4), 529-539.
- [10] Phadke, A. G., Thorp, J. S. (2008). *Synchronized phasor measurements and their applications*. Springer Science & Business Media.
- [11] Giglio, L., Schroeder, W., Justice, C. O. (2016). The collection 6 MODIS active fire detection algorithm and fire products. *Remote Sensing of Environment*, 178, 31-41.
- [12] Jain, P., Coogan, S. C., Subramanian, S. G., Crowley, M., Taylor, S., Flannigan, M. D. (2020). A review of machine learning applications in wildfire science and management. *Environmental Reviews*, 28(4), 478-505.
- [13] Mosavi, A., Ozturk, P., Chau, K. W. (2018). Flood prediction using machine learning models: Literature review. *Water*, 10(11), 1536.
- [14] Ban, Y., Zhang, P., Nascetti, A., Bevington, A. R., Wulder, M. A. (2020). Near real-time wildfire progression monitoring with Sentinel-1 SAR time series and deep learning. *Scientific Reports*, 10(1), 1-15.
- [15] Kundur, P., Paserba, J., Ajjarapu, V., Andersson, G., Bose, A., Canizares, C., ... Vittal, V. (2004). Definition and classification of power system stability IEEE/CIGRE joint task force on stability terms and definitions. *IEEE Transactions on Power Systems*, 19(3), 1387-1401.
- [16] Buldyrev, S. V., Parshani, R., Paul, G., Stanley, H. E., Havlin, S. (2010). Catastrophic cascade of failures in interdependent networks. *Nature*, 464(7291), 1025-1028.
- [17] Pagani, G. A., Aiello, M. (2013). The power grid as a complex network: A survey. *Physica A: Statistical Mechanics and its Applications*, 392(11), 2688-2700.
- [18] Zheng, H., Yuan, J., Chen, L. (2017). Short-term load forecasting using EMD-LSTM neural networks with a Xgboost algorithm for feature importance evaluation. *Energies*, 10(8), 1168.
- [19] Donon, B., Clément, R., Donnot, B., Marot, A., Guyon, I., Schoenauer, M. (2020). Neural networks for power flow: Graph neural solver. *Electric Power Systems Research*, 189, 106547.
- [20] Chen, K., Hu, J., Zhang, Y., Yu, Z., He, J. (2019). Fault location in power distribution systems via deep graph convolutional networks. *IEEE Journal on Selected Areas in Communications*, 38(1), 119-131.
- [21] Baltrušaitis, T., Ahuja, C., Morency, L. P. (2018). Multimodal machine learning: A survey and taxonomy. *IEEE Transactions on Pattern Analysis and Machine Intelligence*, 41(2), 423-443.

- [22] Huang, Y., Xu, J., Hua, H., Wang, N., Hou, Y. (2020). A novel approach for solar power forecasting based on a deep learning ensemble. *IEEE Access*, 8, 28142-28151.
- [23] Panteli, M., Pickering, C., Wilkinson, S., Dawson, R., Mancarella, P. (2017). Power system resilience to extreme weather: Fragility modeling, probabilistic impact assessment, and adaptation measures. *IEEE Transactions on Power Systems*, 32(5), 3747-3757.
- [24] Vugrin, E. D., Castillo, A. R., Silva-Monroy, C. A. (2017). Resilience metrics for the electric power system: A performance-based approach. *Sandia National Lab. (SNL-NM), Albuquerque, NM (United States)*.